Mechanism for high-energy electrons in nonsequential double ionization below the recollision-excitation threshold

Yueming Zhou, Qing Liao, and Peixiang Lu*
Wuhan National Laboratory for Optoelectronics, Huazhong University of Science and Technology, Wuhan 430074, People's Republic of China

(Received 6 April 2009; revised manuscript received 16 May 2009; published 19 August 2009)

High-energy cutoffs for individual electrons from nonsequential double ionization of helium by a 390 nm laser pulse at intensity 0.8 PW/cm^2 have been investigated using a classical 3D ensemble. Below the recollision-excitation threshold, both electrons are bound after recollision and get ionized one by one later. With the trajectory back analyzing of electrons with final energies above $2U_p$, we find an additional mechanism for the latter ionized electron after recollision. Both nuclear and laser forces contribute in this mechanism which leads to a broad transverse momentum distribution.

DOI: 10.1103/PhysRevA.80.023412 PACS number(s): 32.80.Rm, 31.90.+s, 32.80.Fb

I. INTRODUCTION

Nonsequential double ionization (NSDI) of atoms and molecules in intense laser field has been studied extensively during the past three decades since it can provide a profound understanding of laser-matter interaction and electron correlation [1–8]. Now the widely accepted picture for NSDI is well understood by a quasiclassical rescattering model [9]. In this picture, the first electron is ejected near the peak of the electric field, then returns to the singly charged ion as the field changes direction and recollides with the ion inelastically, leading to the second electron ejected in an $(e,2e)$ process or excited and subsequently field ionized [10]. The maximum kinetic energy of the recolliding electron is $3.17U_p$, where $U_p=I/4\omega^2$ is the ponderomotive energy (atomic units are used throughout this paper, unless otherwise stated). At intensities below the recollision threshold I_{t1}, at which $3.17U_p$ equals the ionization potential of the singly charged ion, recollision excitation with subsequent ionization (RESI) mechanism dominates NSDI. The detailed dynamics of RESI has not been fully established, especially if the intensity is below the recollision-excitation threshold I_{t2}, at which $3.17U_p$ equals the energy required to excite the first excited state of the singly charged ion.

Recently, the development of the sophisticated cold target recoil ion momentum spectroscopy and high-repetition-rate lasers provides a useful tool to study the microscopic dynamics of NSDI [11,12]. Two 2007 experiments [13,14] on NSDI of helium at intensities above the recollision threshold have reported significant numbers of electrons from NDSI with momenta along the laser polarization axis above $2\sqrt{U_p}$ and thus energies above $2U_p$. Recoil recollision is the responsible mechanism for high-energy electrons [13]. The importance of the nucleus' role in the recoil recollision is unveiled with three-dimensional (3D) classical ensembles [15,16]. In the intensity range $I<I_{t2}$ and $I_{t2}<I<I_{t1}$, high-energy ($>2U_p$) electrons from NSDI of helium in 390 nm laser pulses have also been reported [17]. With numerical solution of time-dependent Schrödinger equation (TDSE), the authors discovered an intensity-independent cutoff at $5.3U_p$ in the two-electron energy spectrum, which has been confirmed by a very recent experiment on NSDI of Ar below the recollision threshold [18]. By introducing a simple model in which the recollisions are treated as a series of weak electric-field impulses, they verified that the $5.3U_p$ is composed of $1.9U_p$ energy acquired by the struck electron and of $3.4U_p$ delivered by the recolliding electron. With classical 3D ensembles, Haan *et al.* found two important processes that lead to high-energy electrons from NSDI of helium at intensity 1.1 PW/cm^2 [19]. One is the nuclear scattering of the free electron at recollision. The other is an excitation-boomerang-escape sequence in which the electron that is bound after recollision changes velocity sign in the laser polarization axis, escapes over a suppressed barrier. The nucleus plays an important role in the change in phase of electron oscillation relative to the laser phase in both processes. However, in the intensity range $I<I_{t2}$ (I_{t2}=0.9 PW/cm^2), the responsible mechanism for high-energy electrons has not been studied.

In this paper, we exploit the classical 3D ensemble [15,20] to investigate high-energy electrons from NSDI of He by a 390 nm laser pulse at intensity 0.8 PW/cm^2, below I_{t2}. Our simulations reproduce the high-energy cutoff in the two-electron energy spectra and show significant numbers of electrons with energies above $2U_p$. With the trajectory back analyzing, we extract the responsible microscopic dynamics for high-energy electrons. Besides the nuclear scattering at recollision and nuclear boomerang after recollision [19] that lead to the electron with final energy above $2U_p$, in the low intensity regime, we find another responsible mechanism for high-energy electrons, in which the electrons can be accelerated by the laser field for about three consecutive 1/4 cycles near the core after recollision. This process leads to a broad transverse momentum distribution of high-energy electrons.

The paper is organized as follows. In Sec. II we describe the classical ensemble model. In Sec. III, we present our results with discussions. Finally, we shall summarize the paper in Sec. IV.

II. CLASSICAL ENSEMBLE MODEL

This classical model has been successfully in understanding NSDI in the high intensity regime before [15,19–22]. For

*Corresponding author; lupeixiang@mail.hust.edu.cn

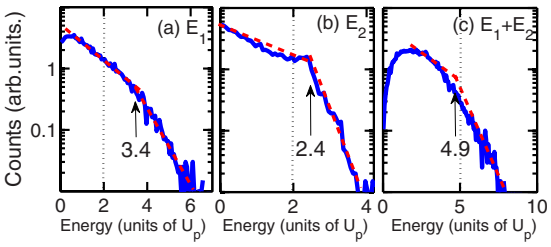

FIG. 1. (Color online) Energy spectra of the (a) first, (b) second electrons, and (c) two-electron for helium double ionization at 0.80 PW/cm^2. The ensemble size is 2.5×10^6 and more than 1.9×10^4 DI trajectories are obtained. The dashed lines are added to guide the eye.

the low intensity we have used in this paper the classical model is also valid because that significant highly excited states are founded after recollision (as discussed below), where there is a pseudocontinuum.

In the classical model, the evolution of the two-electron system is determined by the classical equation of motion: $d^2\mathbf{r}_i/dt^2=-\nabla[V_{ne}(r_i)+V_{ee}(r_1,r_2)]-\mathbf{E}(t)$, where the subscript i is the electron label that runs from 1 to 2 and $\mathbf{E}(t)$ is the electric field, which has a trapezoidal pulse shape with two-cycle turn on, six cycles at full strength, and two-cycle turn off. The potentials are $V_{ne}(r_i)=-2/\sqrt{r_i^2+a^2}$ and $V_{ee}(r_1,r_2)=1/\sqrt{(r_1-r_2)^2+b^2}$, representing the ion-electron and electron-electron interactions, respectively.

To obtain the initial value, the ensemble is populated starting from a classically allowed position for the helium ground-state energy of −2.9035 a.u. The available kinetic energy is distributed between the two electrons randomly in momentum space. Each electron is given radial velocity only, with sign randomly selected [21]. Then the electrons are allowed to evolve a sufficient long time (100 a.u.) in the absence of the laser field to obtain stable position and momentum distributions [21]. To avoid autoionization, the screening parameter a is initially set to be 0.825 [20,21]. Then we change the screening parameter a to 0.4 for both electrons as soon as one electron reaches $r=5.0$ a.u. to increase the influence of ucleus on the dynamics of electrons at and after recollision [15,22]. To conserve energy we offset the decrease in the potential energy of each electron with a kinetic boost for its radial motion [15,22]. The shield parameter b is set to be 0.05 during the whole process.

III. RESULTS AND DISCUSSIONS

Figure 1 shows the energy spectra of the electrons from NSDI of He. With the same definition of energy cutoff as used in [17,18], a $4.9U_p$ cutoff, as indicated by the black arrow in Fig. 1(c), is evident in the two-electron energy spectrum. Further calculations show that this energy cutoff is independent of the laser intensity in the range $I<I_{t2}$. This cutoff is in agreement with the previous theoretical prediction [17] and the experimental result [18]. In order to explore the responsible double ionization (DI) process for this high-energy cutoff, we trace the DI trajectories and find that the most likely scenario for this intensity and wavelength is the

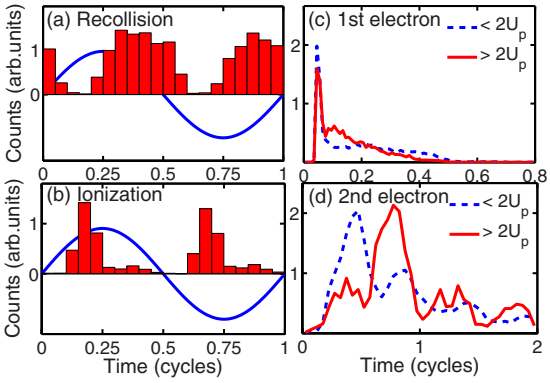

FIG. 2. (Color online) Counts of the trajectories vs laser phase at the time of (a) recollision and (b) final ionization of the second electrons. (c) The time delay between recollision and ionization of the first electrons. (d) The same as (c) but for the second electrons. There are some electrons ionized with time delay more than 2 cycles, but they are not collected in (d). Plots (c) and (d) are normalized so the area under each curve is the same.

production of a doubly exited state after recollision. The two exited electrons are ionized one after the other, thus we classify the electrons based on the ionization time after recollision. We refer to the first and the second ionized electrons after recollision as the first and the second electrons below, respectively. The individual energy spectra of the first and the second electrons are shown in Figs. 1(a) and 1(b), respectively. As indicated by the black arrows, the spectrum of the first electrons exhibits a cutoff around $3.4U_p$ and that of the second electrons exhibits a much more obvious cutoff at $2.4U_p$. With trajectory back analyzing we find that most of the first electrons achieve high energies through either of the two processes proposed in [19].

Next we focus on the second electrons with high energies. For each DI trajectory, the recollision time is defined as the instant of the closest approach of the two electrons after single ionization. We trace the energies of both electrons at 0.04 cycle after recollision and the final ionization time is defined as the instant when the energy of the electron becomes positive for the first time, where the energy of each electron contains the kinetic energy, potential energy of the electron-ion interaction and half electron-electron repulsion. Figures 2(a) and 2(b) show the laser phase at recollision and at final ionization of the second electrons, respectively. In both plots only the trajectories leading to the second electron with final energy above $2U_P$ are collected. Figure 2(c) shows the time delay between the recollision and the final ionization of the first electrons. The solid red curve indicates the first electrons with final energies above $2U_p$ and the dashed blue curve indicates the first electrons with final energies below $2U_p$. Almost all of the first electrons, in spite of its final energy is above or below $2U_p$, are ionized within half a laser cycle after recollision. Figure 2(d) also shows the time delay but for the second electrons. For most of the second electrons with final energies below $2U_p$, the corresponding time delay between recollision and ionization is less than half a cycle. While for most of the second electrons with final energies above $2U_p$, indicated by the sold red curve in Fig. 2(d), the time delay is about 0.75 cycle, exceeding half a cycle.

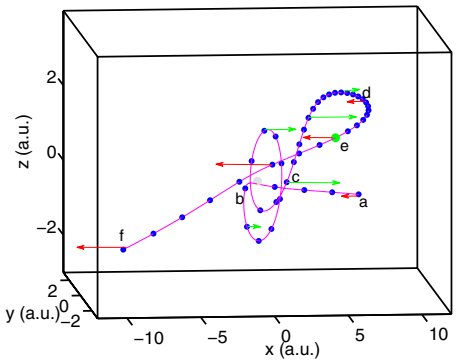

FIG. 3. (Color online) A sample trajectory of the second high-energy electron. The successive dots indicate elapsed time of 0.02 cycle. The electron gets ionized at position e (green dot). The gray dot indicates the doubly charged ion. The red and green arrows indicate the laser force.

The microscopic dynamics of the second electrons with energies above $2U_p$ can be obtained by examining their trajectories. A sample trajectory of one of the second electrons from Fig. 1(b) is plotted in Fig. 3, beginning at $3.44T$ (position a; T is the laser cycle) and ending at $4.34T$ (position f). For this illustrative trajectory, the corresponding recollision occurs at $3.52T$ (at position b) and both electrons are bound after recollision. The first electron, which is not shown in Fig. 3, is ionized through nuclear boomerang [19] at $3.62T$ and achieves final energy of $2.53U_p$, leaving the second electron looping around the core. As the electric field increases up to its maximum, the second electron is pushed away from the core along the positive x axis (the laser polarization is along x axis). During this way (c→d), the nucleus decelerates the electron and makes the sign change of v_x near position d. We refer to this position as turning position below. The electron has gained energy from the laser field for about 1/4 cycle during the way c→d. When the electron's velocity direction changes, the electric force reverses almost at the same time and the electron begins to be accelerated by the combined laser and nuclear force. Therefore, the electron can gain energy from the field again for about two consecutive 1/4 cycles and achieves positive total energy at position $e(t=4.18T)$.

The sequence of events, which is shown in Fig. 4, reveals the time evolution of the energies and the x part of the motion of both electrons. Plot (a) shows the time just before recollision, during which a substantial exchange of energy between the two electrons occurs. After recollision, the first electron, coded in cyan, stays in an excited state with energy −0.2 a.u. and the second electron, coded in blue, with energy −0.6 a.u. The first electron is ionized just after the time shown in plot (b) when its velocity direction is changed by the combined Coulombic and laser force. The second electron begins to be pushed away from the core at plot (c) and gains energy from the laser field before it is stopped by the rising potential barrier at $4.0T$, when its energy has risen to −0.2 a.u. Finally, the electron achieves positive energy when it moves toward the core after the velocity direction change and escapes into the negative x direction. For this particular trajectory, the second electron is ionized with final energy as much as $2.33U_p$.

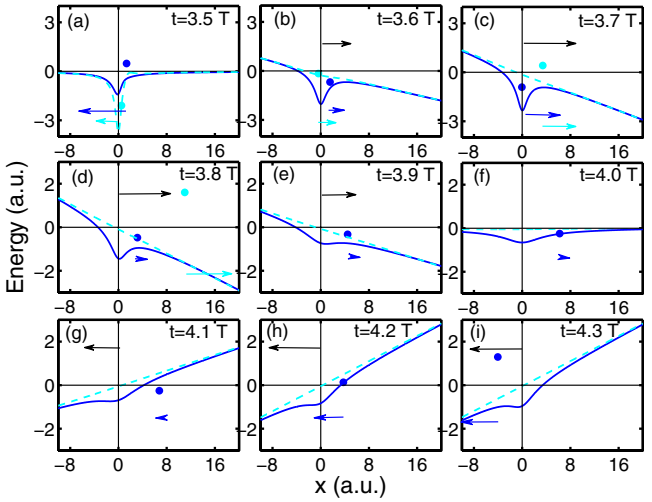

FIG. 4. (Color online) Sequence for the trajectory of Fig. 3. Curves show the potential energies (the combined potential of nucleus, e-e repulsion and laser field) for each electron. The upper black arrows show laser force and the lower cyan (gray) and blue arrows show v_x.

The above analysis reveals that the second electron can gain energy from the laser field for three consecutive 1/4 cycles after recollision. In this process, the electron first moves slowly away from the nucleus near the field maximum and gains energy from the laser field for 1/4 cycle before stopped by the rising potential. When the field decreases to zero and reverses its direction, the velocity of the electron is also reversed by the nuclear Coulombic attraction. Thus, the electron can gain energy from the field again in the next half laser cycle and achieves final energy above $2U_p$. We refer to this process as the laser-assisted nuclear boomerang.

By tracing the trajectories of the second high-energy electrons we find that their turning positions are about 4–8 a.u. from the nucleus. The electron's motion is greatly affected by the nucleus after its velocity direction change at the turning position and the work done on the electron by the laser field during the next half cycle is [19]: $W=\int_{t_0}^{t_f}\mathbf{E}_0\, sin(\omega t)\cdot \boldsymbol{v}(t)dt$, where $\boldsymbol{v}(t)$ is the velocity. $\boldsymbol{v}(t)$ is a nontrivial function of time and thus W should be calculated numerically for different E_0 and ω. For the laser intensity and wavelength we used, an electron that starts from rest in the region $x=4.5-6.5$ a.u. and $y\approx 1.5$ a.u. at a field zero and evolves in the combined laser and Coulombic field can ionize with final energy approximate $2.4U_p$. Note that the electron's final energy depends on the transverse position and velocity at the turning position. An electron that starts from rest at the turning position with $y=0$ and $v_y=0$, can achieve final energy as much as $3.5U_p$. However, trajectory tracing shows that most electrons are pushed away to turning positions with transverse distance of 0.5–2.5 a.u. and few electrons are confined to move along the polarization axis with transverse distance smaller than 0.5 a.u.

Note that the second electron may miss to be pushed away from the core at the first field maximum after recollision and it loops around the core for multiple half cycles before being

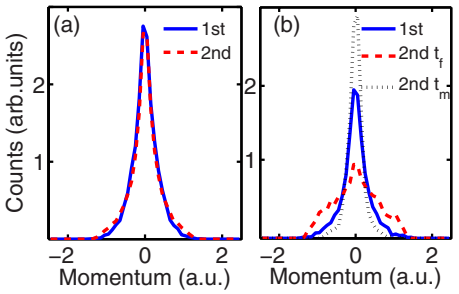

FIG. 5. (Color online) Transverse momentum spectra (P_y) of the first (solid blue curves) and second (dashed red curves) electrons. Only the electrons with final energy below and above $2U_p$ are collected in (a) and (b), respectively. The dotted blank curve in (b) indicates the transverse momentum of the second high-energy electrons when they reach the turning positions. Plot for the other component (P_z) would look like the same. Both plots are normalized so that the area under each curve is the same.

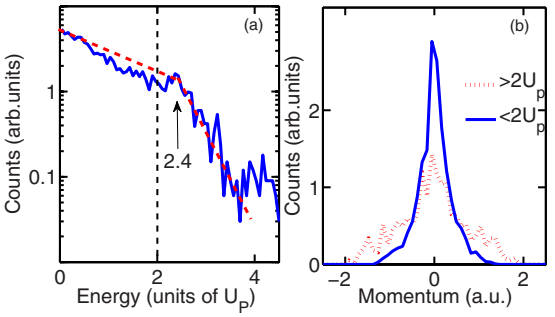

FIG. 6. (Color online) The energy spectrum (a) and the transverse momentum spectra (b) of the second electron. The laser parameter is the same as that in Fig. 1, but the final screening parameter is $a=0.1$. The solid blue and the dashed red curves of (b) indicate the transverse momentum of the second electrons with final energy lower than $2U_p$ and higher than $2U_p$, respectively.

pushed away. These electrons are ionized with time delay more than 0.75 cycle [see Fig. 2(d)]. There are also some other processes that lead to the second electron with final energy above $2U_p$. For example, backscattering after multiple collisions, nuclear scattering of the free returning electron [23]. However, laser-assistant nuclear boomerang is the primary process responsible for the second high-energy electrons. Our statistics reveals that 80% of the second electrons with energies above $2U_p$ experience this process.

A recent study [22] on the back-to-back electron emission from NSDI of helium by laser at 483 nm and intensity 0.5 PW/cm^2 has also shown that either the first or the second electron can achieve final energies above $2U_p$ (see Fig. 4 of Ref. [22]). The authors show that a significant part of the second electrons especially for the back-to-back emission trajectories are ionized with time delay about 0.75 cycle. Thus laser-assisted nuclear boomerang is the responsible process for the second high-energy electrons with time delay about 0.75 cycle in that study.

The transverse momentum spectra of the DI electrons are shown in Fig. 5. The solid blue curve and dashed red curve in Fig. 5(a) indicate transverse momenta of the first and the second low-energy ($<2U_p$) electrons, respectively. The solid blue curve in Fig. 5(b) indicates the first high-energy electrons. All of the spectra are narrow and consistent with the previous study on NSDI of Ar and Ne in the low intensity regime [24]. However, the transverse momentum spectrum of the second high-energy electrons, which is shown by the dashed red curve in Fig. 5(b), is much broader. This provides an evidence that the second high-energy electrons ionize through a different process. How do these electrons obtain larger transverse momenta? We trace the trajectories and extract the transverse momenta of the second high-energy electrons when they reach turning positions. The spectrum is shown by the dotted blank curve in Fig. 5(b). It clearly shows that the momentum distribution is even narrower than that of the first high-energy electrons. This means that the second electrons also favor small transverse momenta when they are pushed away at the field maximum when the barrier is suppressed. The transverse momentum is not affected by the laser field and Coulombic force when the electron moves beyond the area where the ion core potential is effective. Therefore, we conclude that the larger transverse momenta are obtained when the electrons pass by the nucleus after the velocity direction change at turning positions. During this process the time taken by the electron to move from the turning position to the other side of the core is significant, and the transverse attraction of the nucleus on the electron is very strong. As a consequence, the electron gains considerable transverse momentum.

We have investigated NSDI for a smaller value ($a=0.1$) of the final screening parameter. The energy spectrum and the transverse momentum spectra of the second electrons are shown in Figs. 6(a) and 6(b), respectively. The energy spectrum also shows a evident cutoff at $2.4U_p$, and the second high-energy electrons also exhibit a broad transverse momentum distribution. Back tracing shows that the ionization processes of the second electrons are not changed: most of the second electrons achieve high energies through laser-assisted nuclear boomerang. This is not surprising because the soft-core potentials with screening parameters $a \leq 0.4$ are similar and very close to the bare Coulomb potential (not shown here). Thus the soft-core potential ($a=0.4$) is a good approximation to the bare Coulomb potential and the ionization processes of the second electrons will not change with the value of a when a is small.

Throughout this paper the analysis is based on the tunneling or over-the-barrier ionization mechanism, and the multiphoton process is neglected. The reasons are as follows. Before recollision, in our calculation the ponderomotive energy $U_p=0.416$ a.u. and the first ionization potential of helium is $I_p=0.9$ a.u., the Keldysh parameter $\gamma=\sqrt{I_p/2U_p}\simeq 1$. It is at the boundary between the multiphoton and tunneling regimes for the single ionization of helium. However, for the intensity we used the potential barrier is strongly suppressed by the laser field (shown in Fig. 7) and the electrons' energies are often higher than the barrier which leads to the electrons ionize over the barrier. Additionally, after recollision the binding energies of the first and the second excited electrons are approximate 0.25 and 0.6 a.u., respectively. The Keldysh parameters for this system are less than $1(\gamma_1=\sqrt{0.25/2U_p}=0.55, \gamma_2=\sqrt{0.6/2U_p}=0.85)$, and the energies of both electrons are well above the suppressed barrier. As a conse-

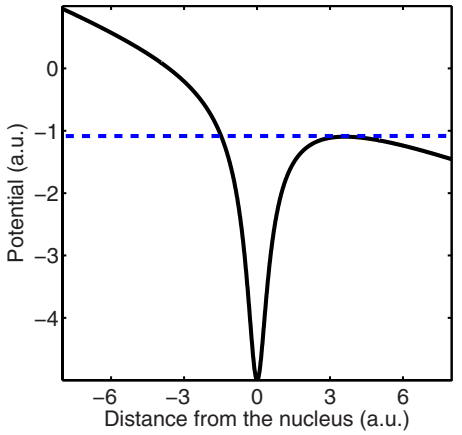

FIG. 7. (Color online) Combined soft-core and electric field potential $V(z)=-2/\sqrt{a^2+z^2}+Ez$, where a=0.4. The intensity of the laser field is 0.8 $\mathrm{PW/cm^2}$.

quence, tunneling or over-the-barrier ionization process dominates both the single ionization of helium before recollision and the ionization of the doubly excited system after recollision for the intensity we used.

IV. SUMMARY

In conclusion, we have investigated the microscopic process of generation of high-energy electrons from NSDI of helium for laser wavelength 390 nm at intensities below the recollision-excitation threshold with the classical 3D ensemble. The high-energy cutoff in the two-electron energy spectrum has been reproduced. Besides the nuclear backscattering and nuclear boomerang, we have found another dominant mechanism that leads to high-energy electrons, which is referred as laser-assisted nuclear boomerang. This mechanism, almost absent in NSDI for intensities above the recollision-excitation threshold, becomes more dominant as the intensity further decreases. In addition, it leads to high-energy electrons with a large transverse momentum distribution. This feature may be used to identify this mechanism in future experiments on NSDI at intensities below the recollision-excitation threshold.

ACKNOWLEDGMENTS

We thank Dr. S. L. Haan for enthusiastic help in the 3D ensemble program. This work was supported by the National Natural Science Foundation of China under Grants No. 10774054 and No. 10734080, the specialized Research Fund for the Doctoral Program of Higher Education of China under Grant No. 20040487023, and the National Key Basic Research Special Foundation under Grant No. 2006CB806006.

[1] B. Walker, B. Sheehy, L. F. DiMauro, P. Agostini, K. J. Schafer, and K. C. Kulander, Phys. Rev. Lett. **73**, 1227 (1994).
[2] J. B. Watson, A. Sanpera, D. G. Lappas, P. L. Knight, and K. Burnett, Phys. Rev. Lett. **78**, 1884 (1997).
[3] M. Lein, E. K. U. Gross, and V. Engel, Phys. Rev. Lett. **85**, 4707 (2000).
[4] A. Becker and F. H. M. Faisal, Phys. Rev. Lett. **84**, 3546 (2000).
[5] Th. Weber *et al.*, Phys. Rev. Lett. **84**, 443 (2000).
[6] R. Moshammer *et al.*, J. Phys. B **36**, L113 (2003).
[7] M. Weckenbrock *et al.*, Phys. Rev. Lett. **92**, 213002 (2004).
[8] Q. Liao, P. Lu, Q. Zhang, W. Hong, and Z. Yang, J. Phys. B **41**, 125601 (2008).
[9] P. B. Corkum, Phys. Rev. Lett. **71**, 1994 (1993).
[10] B. Feuerstein *et al.*, Phys. Rev. Lett. **87**, 043003 (2001).
[11] J. Ullrich *et al.*, Rep. Prog. Phys. **66**, 1463 (2003).
[12] Y. Liu *et al.*, Opt. Express **15**, 18103 (2007).
[13] A. Staudte *et al.*, Phys. Rev. Lett. **99**, 263002 (2007).
[14] A. Rudenko, V. L. B. de Jesus, T. Ergler, K. Zrost, B. Feuerstein, C. D. Schroter, R. Moshammer, and J. Ullrich, Phys. Rev. Lett. **99**, 263003 (2007).
[15] S. L. Haan, J. S. Van Dyke, and Z. S. Smith, Phys. Rev. Lett. **101**, 113001 (2008).
[16] D. F. Ye, X. Liu, and J. Liu, Phys. Rev. Lett. **101**, 233003 (2008).
[17] J. S. Parker, B. J. S. Doherty, K. T. Taylor, K. D. Schultz, C. I. Blaga, and L. F. DiMauro, Phys. Rev. Lett. **96**, 133001 (2006).
[18] Y. Liu, S. Tschuch, A. Rudenko, M. Durr, M. Siegel, U. Morgner, R. Moshammer, and J. Ullrich, Phys. Rev. Lett. **101**, 053001 (2008).
[19] S. L. Haan and Z. S. Smith, Phys. Rev. A **76**, 053412 (2007).
[20] S. L. Haan, L. Breen, A. Karim, and J. H. Eberly, Phys. Rev. Lett. **97**, 103008 (2006).
[21] S. L. Haan, L. Breen, A. Karim, and J. H. Eberly, Opt. Express **15**, 767 (2007).
[22] S. L. Haan, Z. S. Smith, K. N. Shomsky, and P. W. Plantinga, J. Phys. B **41**, 211002 (2008).
[23] B. Walker, B. Sheehy, K. C. Kulander, and L. F. DiMauro, Phys. Rev. Lett. **77**, 5031 (1996).
[24] E. Eremina *et al.*, J. Phys. B **36**, 3269 (2003).